

12.5 Gbit/s carrier-depletion based silicon Mach-Zehnder modulator with a 2 V driven voltage

H. Yu,¹ W. Bogaerts,¹ K. Komorowska,¹ J. V. Campenhout,² P. Verheyen,² P. P. Absil,² and R. Baets¹

¹ Dept. of Information Technology, Ghent University-imec, Center for Nano- and Biophotonics (NB Photonics), St.-Pietersnieuwstraat 41, 9000 Gent, Belgium
² imec, Kapeldreef 75, 3001 Leuven, Belgium

We demonstrate a carrier-depletion based silicon optical modulator with a figure of merit of 1.3 V-cm. The device is based on a Mach-Zehnder interferometer whose two arms incorporate lateral PN junctions and lumped electrodes. With a 3mm phase shifter, the modulator can be driven by a signal of 2 V peak-to-peak voltage. The modulation depths at 5 Gbit/s, 10 Gbit/s and 12.5 bit/s are 5.92 dB, 4.51 dB and 3.73 dB, respectively. The total insertion loss of the device is 8 dB.

Introduction

A power efficient and high-speed silicon modulator is a key building block in optical interconnects which can overcome the bottleneck of current electrical interconnect systems. Various silicon optical modulations have been demonstrated during the last decade based on different effects [1]. Among these candidates the carrier-depletion based modulator is the most common scheme due to its CMOS compatibility, fabrication simplicity and high operation speed. This structure incorporates a PN junction inside a silicon waveguide and manipulates the refractive index of silicon by reverse biasing the PN junction. However, as a result of the small overlap between the carrier depletion region and the optical mode, the carrier-depletion based modulator exhibits poor modulation efficiency provided that a Mach-Zehnder (MZ) interferometer is used to convert the refractive index modulation to the optical intensity modulation. Therefore a large driving voltage is necessary which cannot be generated directly by a CMOS driver circuit. An alternative is to enhance the interaction between the carrier depletion region and the optical mode by an optical resonator. In order to make the resonator operate at the right wavelength, a thermal tuner together with a control circuit is required which increase complexity of the system. In this paper, we cut the driving voltage of carrier-depletion based silicon MZ modulator by adjusting the length of the phase shifter. With a phase shifter of 3 mm, the modulator can be driven by a voltage swing of 2 V_{pp} up to 12.5 Gbit/s.

Device design and fabrication

The device is an asymmetrical MZ interferometer with a path difference of 40 μm. Two compact 1×2 multi-mode interferometers (MMI) are used to split and combine the beam. The phase shifter on each arm of the MZ interferometer is formed by embedding a lateral PN junction in a rib waveguide. Schematic 3D and top views of the phase shifter are presented in Fig. 1. The width and height of the rib waveguide are 500 nm and 220 nm respectively. The slab height is 150 nm in order to be compatible with the

- [2] L. H. Frandsen, P. I. Borel, Y. X. Zhuang, A. Harpøth, M. Thorhaage, M. Kristensen, W. Bogaerts, P. Dumon, R. Baets, V. Wiaux, J. Wouters, and S. Beckx, "Ultra-low-loss 3-dB photonic crystal waveguide splitter," *Optics Letters*, vol. 29, 1623-1625, 2004.
- [3] W. Bogaerts, P. Dumon, D. Van Thourhout, and R. Baets, "Low-loss, low-cross-talk crossings for silicon-on-insulator nanophotonic waveguides," *Optics Letters*, vol. 32, 2801-2803, 2007.
- [4] P. D. Trinh, S. Yegnanarayanan, B. Jalali, "Integrated optical directional couplers in silicon-on-insulator," *Electronics Letters*, vol. 31, 2097-2098, 1995.
- [5] M. W. Geis, S. J. Spector, R. C. Williamson, T. M. Lyszczarz, "Submicrosecond submilliwatt silicon-on-insulator thermo-optic switch," *IEEE Photonics Technology Letters*, vol. 16, 2514-2516, 2004.
- [6] A. Liu, L. Liao, D. Rubin, H. Nguyen, B. Ciftcioglu, Y. Chetrit, N. Izhaky, and M. Paniccia, "High-speed optical modulation based on carrier depletion in a silicon waveguide," *Optics Express*, vol. 15, 660-668, 2007.
- [7] Y.-H. Kuo, H. Rong, V. Sih, S. Xu, M. Paniccia, and O. Cohen, "Demonstration of wavelength conversion at 40 Gb/s data rate in silicon waveguides," *Optics Express* 14, 11721-11726, 2006.
- [8] J. Brouckaert, W. Bogaerts, P. Dumon, D. Van Thourhout, and R. Baets, "Planar concave grating demultiplexer fabricated on a nanophotonic silicon-on-insulator platform," *IEEE Journal of Lightwave Technology*, vol. 25, 1269-1275, 2007.
- [9] J. Liu, M. Beals, A. Pomerene, S. Bernardis, R. Sun, J. Cheng, L. C. Kimerling, and J. Michel, "Waveguide-integrated, ultralow-energy GeSi electro-absorption modulators," *Nature Photonics*, vol. 2, 433-437, 2008.
- [10] J. Michel, J. Liu, and L. C. Kimerling, "High-performance Ge-on-Si photodetectors," *Nature Photonics*, vol. 4, 527-534, 2010.
- [11] D. Liang, and J. E. Bowers, "Photonic integration: Si or InP substrates?," *Electronics Letters*, vol. 45, 2009.
- [12] O. Boyraz, and B. Jalali, "Demonstration of a silicon Raman laser," *Optics Express*, vol. 12, 5269-5273, 2004.
- [13] H. Rong, S. Xu, Y. Kuo, V. Sih, O. Cohen, O. Radaay, and M. Paniccia, "Low-threshold continuous-wave Raman silicon laser," *Nature Photonics*, vol. 1, 725-728, 2005.
- [14] J. Liu, X. Sun, R. C.-Aguilera, L. C. Kimerling, and J. Michel, "Ge-on-Si laser operating at room temperature," *Optics Letters*, vol. 35, 679-681, 2010.
- [15] L. Liu, R. Kumar, K. Huybrechts, T. Spuesens, G. Roelkens, E.-J. Geluk, T. de Vries, P. Regreny, D. Van Thourhout, R. Baets, and G. Morthier, "An ultra-small, low-power, all-optical flip-flop memory on a silicon chip," *Nature Photonics*, vol. 4, 182-187, 2010.
- [16] R. Kumar, L. Liu, G. Roelkens, E.-J. Geluk, T. de Vries, F. Karouta, P. Regreny, D. Van Thourhout, R. Baets, and G. Morthier, "10GHz All-Optical Gate Based on a III-V/SOI Microdisk," *IEEE Photonics Technology Letters*, 22, 981-983, 2010.
- [17] L. Liu, J. Van Campenhout, G. Roelkens, R. A. Soref, D. Van Thourhout, P. R. Romeo, P. Regreny, C. Seassal, J.-M. Fedeli, and R. Baets, "Carrier-injection-based electro-optic modulator on silicon-on-insulator with a heterogeneously integrated III-V microdisk cavity," *Optic Letters*, vol. 33, 2518-2520, 2008.
- [18] L. Liu, G. Roelkens, T. Spuesens, R. Soref, P. Regreny, D. Van Thourhout, and R. Baets, "Low-power electro-optical switch based on a III-V microdisk cavity on silicon-on-insulator circuit," in *Proceedings of the Asia Communications and Photonics Conference (ACP)*, 76310P-76310P-6, 2009.
- [19] R. Kumar, T. Spuesens, P. Mechet, P. Kumar, O. Raz, N. Olivier, J.-M. Fedeli, G. Roelkens, R. Baets, D. Van Thourhout, and G. Morthier, "Ultrafast and bias-free all-optical wavelength conversion using III-V-on-silicon technology," *Optics Letters*, vol. 36, 2450-2452, 2011.
- [20] T. Spuesens, D. Van Thourhout, P. Rojo-Romeo, P. Regreny, and J.-M. Fedeli, "CW operation of III-V microdisk lasers on SOI fabricated in a 200 nm CMOS pilot line," in *Proceedings of Group IV photonics*, 199-201, 2011.

processing of the fiber grating coupler. The thickness of the buried oxide layer is $2\ \mu\text{m}$. The doping pattern in Fig. 1 is optimized so as to reduce the optical loss without impairing the modulation efficiency and the operation speed [2]. The nominal doping concentration is $1e18/\text{cm}^3$ for both P and N type silicon, while the P+++ and N+++ regions which reside $1\ \mu\text{m}$ away from the rib edge are heavily doped to $1e20/\text{cm}^3$ in order to form the ohmic contact. The width w of the two strips which form the PN junction in the centre of the waveguide is $300\ \text{nm}$. The pitch L of periodically loaded bridges between the PN junction and the heavily doped contacting area is $1000\ \text{nm}$. Lumped electrodes with GSG pads are used to drive the two phase shifters.

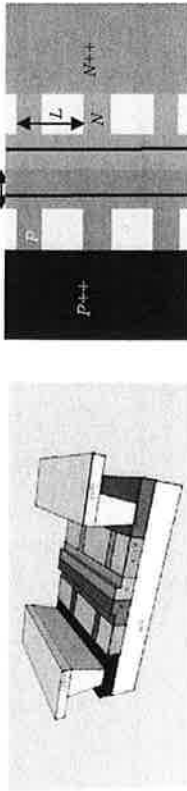


Fig. 1. Schematic 3D (left) and top (right) views of the phase shifter

The optical modulator was fabricated on $200\ \text{mm}$ SOI wafers. $193\ \text{nm}$ optical lithography and silicon dry etching were used to define the optical waveguide. The implantation window was opened by $248\ \text{nm}$ lithography. Subsequently ion implantation was carried out with a sweep of different implantation conditions in the wafer matrix so as to optimize it. After that a thin layer of Ni was deposited using an oxide hard mask to form a local silicide. This was followed by wafer dicing. The diced sample was spin coated with a BCB layer. After via etching through the BCB, a Pt/Au electrode was patterned by the lift-off technology.

Static and dynamic measurement

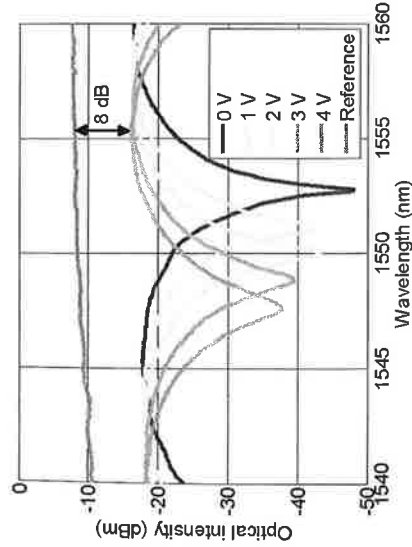


Fig. 2. Transmission spectrum of the modulator for different reverse biases

The transmission spectra of the asymmetrical MZ modulator as a function of the wavelength are shown in Fig. 2 for different reverse biases. What is shown together is the spectrum of the reference straight waveguide with the same length. The figure of

merit $V_{\pi}L_{\pi}$ of the modulator can be extracted from the spectral shift and the free spectrum range (FSR), whose value is $1.32\ \text{V}\cdot\text{cm}$ for a reverse bias from $0\ \text{V}$ to $1\ \text{V}$. This value slightly degrades to $1.68\ \text{V}\cdot\text{cm}$ if we compare the spectrums of $0\ \text{V}$ and $4\ \text{V}$. The on-chip insertion loss of the modulator is $8\ \text{dB}$ which includes a loss of $1.5\ \text{dB}$ from $2\ \text{MMIs}$ and $4\ \text{rib/wire}$ waveguide transitions. We estimate that loss of the phase shifter itself is about $2.2\ \text{dB}/\text{mm}$.

The dynamic measurement is carried out by driving the modulator with a pseudorandom bit sequence (PRBS) of 2^{-1} pattern length. The $2\ V_{pp}$ PRBS output of the pulse pattern generator is sent to the modulator by a GSG probe without any RF amplification. A bias tee is used to add a DC bias voltage to the RF signal. Before being sent to the digital communication analyser, the optical output from the modulator passes through an EDFA and a band pass tuneable filter. Eye diagrams obtained at $5\ \text{Gbit/s}$, $8\ \text{Gbit/s}$, $10\ \text{Gbit/s}$ and $12.5\ \text{Gbit/s}$ are presented in Fig. 3 where the optical wavelength and the DC reverse bias are fixed at $1550\ \text{nm}$ and $5.3\ \text{V}$ respectively. Clear eye open is observed up to $12.5\ \text{Gbit/s}$ which is the upper limit of our measurement system. The extinction ratio at $5\ \text{Gbit/s}$, $8\ \text{Gbit/s}$, $10\ \text{Gbit/s}$ and $12.5\ \text{Gbit/s}$ are $5.92\ \text{dB}$, $4.88\ \text{dB}$, $4.51\ \text{dB}$ and $3.73\ \text{dB}$ respectively.

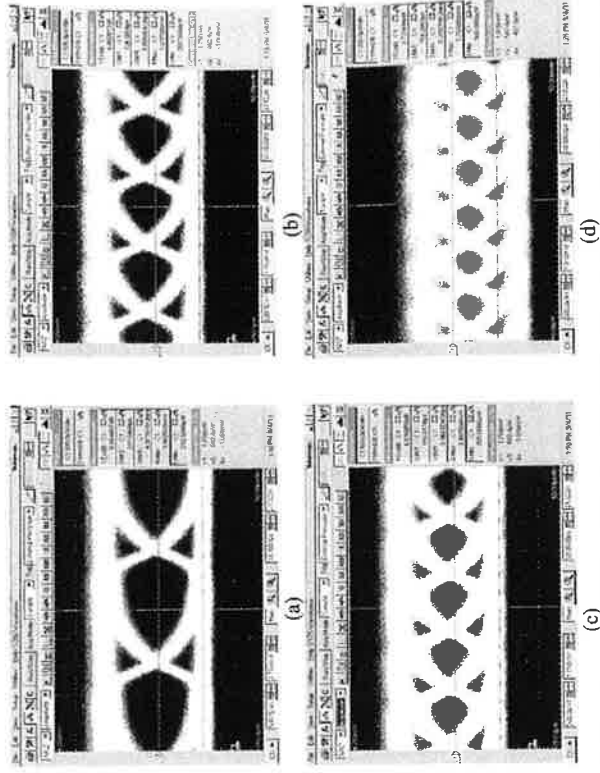


Fig. 3. Eye diagrams at different bit rates: (a) $5\ \text{Gbit/s}$ (a), (b) $8\ \text{Gbit/s}$, (c) $10\ \text{Gbit/s}$ (d) $12.5\ \text{Gbit/s}$

Conclusion

It is well known that for a MZ modulator the phase shifter length determines the modulation speed because of the RC constant, so most reported MZ modulators resort to short phase shifters for $10\ \text{Gbit/s}$ operation when they are driven by a lumped electrode [3-5]. This approach imposes a high requirement on the driven voltage ($V_{pp} > 5\ \text{V}$) in order to have sufficient modulation depth. In this paper we show that with a lumped electrode, a phase shifter as long as $3\ \text{mm}$ could still supports a bit rate of up to $12.5\ \text{Gbit/s}$. Due to the long phase shifter, the modulator can be driven by a signal with

2 V_{pp} voltage swing. Further experiment result show that the operation speed can be boosted to 40 Gbit/s by a travelling wave electrode.

References

- [1] G. T. Reed, G. Mashanovich, F. Y. Gardes and D. J. Thomson, "Silicon optical modulators," *Nature Photon.* vol. 48, 518-526, 2010.
- [2] H. Yu, W. Bogaerts, and A. D. Keersgieter, "optimization of ion implantation condition for depletion-type silicon optical modulators," *IEEE J. Quantum Electron.* vol. 46, 1763-1768, 2010.
- [3] M. R. Watts, W. A. Zortman, D. C. Trotter, R. W. Young and A. L. Lentine, "Low-voltage, compact, depletion-mode, silicon Mach-Zehnder modulator," *IEEE J. Sel. Top. Quantum Electron.* vol. 16, 159-164, 2010.
- [4] G. Rasigade, D. M. Morini, M. Ziebell, J. M. Fédéli, F. Milesi, P. Grosse, E. Cassan, and L. Vivien, "10 Gbit/s silicon optical modulator with 8 dB extinction ratio," in *Proceedings of 8-th IEEE International Conference on Group IV Photonics*, 269-271, 2011.
- [5] N. N. Feng, S. Liao, D. Feng, P. Dong, D. Zheng, H. Liang, R. Shafiqha, G. Li, J. E. Cunningham, A. V. Krishnamoorthy, and M. Asghari, "High speed carrier-depletion modulators with 1.4 V-cm V_L integrated on 0.25 μ m silicon-on-insulator waveguides," *Opt. Express.* vol. 18, 7994-7999, 2010.

Analysis of the performance of InAs/InP(100) quantum dot waveguide photodetectors using a rate equation model

Y. Jiao^{1,2}, B.W. Tilma¹, J. Kotani¹, R. Nötzel¹, M.K. Smit¹ and E.A.J.M. Bente¹

¹ COBRA, Eindhoven University of Technology, The Netherlands

² Centre for Optical and Electromagnetic Research, Zhejiang University, China

In this contribution we present a rate equation model for the simulation of InAs/InP(100) quantum dots which are used as the active material of waveguide photodetectors. Unlike the normal rate equation models in literature which are built for carrier injection and photon emission, our model is modified for the carrier extraction and photon absorption. The simulation results are compared with previous experimental results. Experimental observations are explained in terms of fundamental properties of the quantum dots, e.g. the bias voltage dependent carrier extraction rate and absorption coefficient.

Introduction

In optical coherence tomography (OCT) the wavelength range from 1.6 μ m to 1.8 μ m is of interest for medical and biological applications. This range lies in between two strong water absorption peaks and due to the longer wavelength compared to what is commonly used in OCT, the imaging depth can be improved since the scattering of light is reduced [1].

The photodetector is one of the key components in an OCT system. It detects the output signal from the Michelson interferometer in the OCT set-up. For application of the 1.6 to 1.8 μ m wavelength range in OCT, a photodetector is required to be sufficiently sensitive to these wavelengths. We have used InAs quantum dots (QDs) on InP(100) as the active material for the photodetectors. The average size of the QDs in this material was tuned for a peak optical gain around 1.7 μ m. In our previous study [2] these QD photodetectors have shown good performance in the 1.6 μ m to 1.8 μ m wavelength range.

To interpret and analyze the measurement results a theoretical model based on rate equations was set up. The model is based on a QD optical amplifier model where the current extraction has been included. The responsibilities of several real devices have been calculated and compared to the measurement results. The spectral response as well as the absorption behavior of the QDs have also been simulated and will be discussed.

QD rate equation model

Various rate equation models have been proposed for understanding the gain properties of the QD semiconductor optical amplifiers (QD-SOAs) and lasers [3, 4, 5] and such models are used for the analysis of the relation between injected current and gain. In this contribution we present a rate equation model based on a QD-SOA model [3, 5] that has been modified for the simulation of photodetection with current extraction mechanism. In the previous work, a rate equation model has been applied to the analysis of the gain of the QD-SOAs in the 1.6 μ m to 1.8 μ m wavelength range [3]. A good match was



Proceedings of the
2011 Annual Symposium of the
IEEE Photonics Benelux Chapter



Editors

Peter Bienstman, Geert Morthier,
Gunther Roelkens & Marie Verbist



**1 & 2 December 2011
Ghent University
Belgium**

ISBN 9789076546001

IEEE Photonics Benelux Chapter

<http://www.photonics-benelux.org/>

Ghent University

Department of Information Technology (INTEC)

Photonics Research Group